

Dynamics of flexible slender cylinders in axial flow

Part 2. Experiments

By M. P. PAIDOUSSIS

Chalk River Nuclear Laboratories, Atomic Energy of Canada Limited

(Received 12 July 1965 and in revised form 21 March 1966)

The experiments described here were designed to illustrate the dynamical behaviour of flexible cylinders in axial flow theoretically examined in Part 1. Rubber cylinders, either clamped or pinned at the upstream end and free at the other, or pinned at both ends, displayed both buckling and oscillatory instabilities when immersed in flowing water of sufficiently high velocity. The conditions of neutral stability were determined in a number of cases and compared with theory. The observations were in substantial agreement with the theory.

1. Introduction

The aim of the experiments was twofold: first, to study the dynamical behaviour of flexible cylinders in axial flow and, if possible, to reproduce experimentally the buckling and oscillatory instabilities predicted by the theory presented in part 1 (Paidoussis 1966); secondly, to measure the limits of stability in a number of cases, and compare them with the theoretical values.

We consider circular cylinders of cross-sectional area S , length L , weight m per unit length and flexural rigidity EI , in a fluid of density ρ flowing with velocity U parallel to the rest position of the cylinder axis. The cylinders are either supported at both ends or with the downstream end free. In the latter case, the cylinder is terminated at the free end by a short tapering piece of length l which is much smaller than the overall length L . The motions of the cylinder are supposed to be confined in a horizontal plane, so that gravity is not operative. In Part 1 it was found convenient to describe the system in terms of a number of dimensionless 'system parameters' and the dimensionless flow velocity $u = (M/EI)^{1/2}UL$, where M is the virtual mass of the fluid per unit length, which is equal to ρS . The system parameters are $\beta = M/(M + m)$, $\epsilon = L/D$, the coefficients of friction in the normal and axial directions c_N and c_T respectively, and some others which have meaning only for specific conditions of end support. Thus, if both ends are supported, we have $\Gamma = T_0 L^2/EI$, where T_0 is the tension applied externally by moving the supports apart. If the downstream end is free, on the other hand, we have the parameter f , which is essentially a measure of the slenderness of the tapered end-piece (cf. boundary conditions, § 2, part 1), the geometric parameter

$$\chi = (1/S^2L) \int_{L-l}^L S(x) dx,$$

and the coefficient of form drag acting at the free end, c'_T .

It was found in part 1 that, as the flow velocity increases, the system is subject to buckling instability in its first mode and, at higher flow velocities, to oscillatory instabilities in its higher modes. The dimensionless, critical flow velocities u_c at which these instabilities occur depend only on the system parameters defined above. It was found that for buckling and second-mode oscillatory instability the values of u_c are generally in the range $1 < u_c < 10$. To obtain an appreciation of the dimensional flow velocities involved, let us consider a steel cylinder with $L/D = 20$ in water. We suppose that $u_c = 2$, and writing $u_c = 4(\rho/E)^{1/2}(L/D)U_c$ we obtain $U_c \approx 1180$ ft./sec. Even if the cylinder is hollow with wall thickness to diameter ratio of $1/50$, we obtain $U_c \approx 470$ ft./sec. These are substantial flow velocities, not commonly encountered in practice, which may partly explain why the instabilities considered here have apparently not been observed hitherto. For instabilities to occur at more reasonable flow velocities, clearly $1/\rho$ and E must be as small as possible. Accordingly, all the experiments described here were conducted with rubber cylinders in water flow; E in this case was sufficiently small for U_c to be 50 to 100 times less than the values quoted above.

Systematic experiments were conducted with cylinders clamped at the upstream end and free at the other, and with cylinders pinned at both ends. Some observations were also made on cylinders pinned at the upstream end and free downstream.

2. Apparatus

The apparatus consisted of a water-circulating rig with a section in which the various test cylinders could be mounted horizontally. Flow straighteners were placed ahead of the test section in order to eliminate secondary flows and appropriate devices were used for smoothing the pump delivery pressure. The supported ends of the flexible cylinders were anchored on slender struts, great care being taken to avoid flow separation ahead of the test section. The test section with a clamped-free cylinder in position is shown diagrammatically in figure 1. Later some experiments were conducted in another rig where the test section was made from a Perspex block of square cross-section in which was machined a 4 in. diameter flow passage. This arrangement afforded observation of the cylinder inside with minimum visual distortion, and the photographs included here have been taken in this test section.

For some of the early experiments the flexible cylinders were made by cutting a rubber tube into small segments which were subsequently rotated with respect to adjacent segments and glued together, in such a way as to eliminate the permanent bow which is found in commercially available rubber tubing. The outside surface of the composite cylinder was then ground to a uniform diameter. For most experiments, however, the cylinders were cast from liquid silicon rubber ('Silastic'), which hardens into an elastic solid with the aid of a catalyst.

For experiments with clamped-free cylinders, tapered plastic end-pieces of the same specific gravity as the cylinder were glued to the free end. For pinned-pinned cylinders, very short tapered ends were glued to the flexible

cylinder and were connected to the fixed struts on either side of the cylinder by thin, narrow, polythene strips. These strips were glued into slots machined in the tapered end-pieces and the struts; the unsupported length of strip was just long enough to allow flexure. The strips were mounted in the vertical plane, so that the preferred motion of the cylinder was in the horizontal plane. In some cases, horizontally mounted metal strips were used which were soldered on to the struts and pinned in the tapered end-pieces. The downstream strut could be moved axially before the flow was turned on, so as to apply tension to the flexible cylinder if desired; once the flow was turned on, however, no further motion of this support was possible.

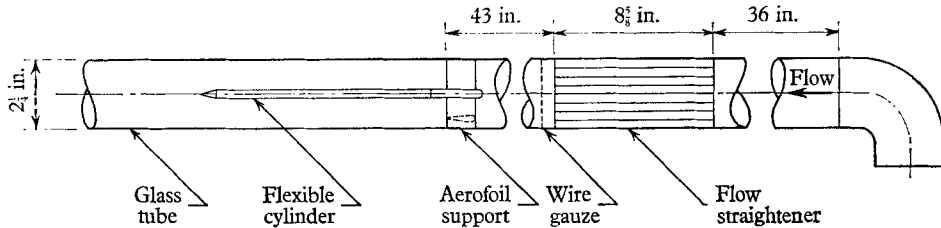


FIGURE 1. Schematic diagram of experimental apparatus.

In most experiments with clamped-free cylinders a thin metal strip was embedded in the cylinder along its length, in the vertical plane of symmetry, effectively limiting all motion to the horizontal plane. The metal strip also provided additional support in the vertical plane in cases where the weight of the cylinder was considerably greater, or smaller, than that of the displaced water. Cylinders with both ends pinned were not fitted with a metal strip, so that the development of instability would not be impeded by excessive resistance to axial extension.

The theoretical problem was formulated on the assumption that there is no variation in the flow velocity U in any plane perpendicular to the cylinder. For the flow velocities at which instabilities were observed, the flow was turbulent and, therefore, except near the pipe wall and the disturbed region near the cylinder itself, the flow velocity across the test section was considered to be nearly uniform. The disturbance in the flow caused by small motions of the cylinder about the position of rest is considered to be negligible. The pressure drop in the length of the cylinder was very small. Hence, it was assumed that the flow velocity across the test section was uniform all along the cylinder, at least to the point of onset of instability. Clearly, however, if a large-scale motion should establish itself, this assumption could no longer be maintained.

3. General observations

In each test, the flow velocity was increased in small steps, starting from zero; at each step, time was allowed for spontaneous development of instability.

Considering clamped-free cylinders first, it was found that, at small flow velocities, small random vibrations were always damped. At sufficiently high flow velocities, however, the system became unstable provided that (a) the free end tapered smoothly, and (b) the cylinder was not too long; or, in terms of our

theoretical parameters, provided that f was not too small nor ϵ too large. If these conditions were met, as the flow velocity increased, the system first buckled and then spontaneously developed second-mode unstable oscillation. At still higher flow velocities, third-mode unstable oscillation was observed. The shape of the buckled cylinder was very similar to that of a beam deflected in its first mode; the shape of a cylinder when performing amplified oscillations is shown in figure 2(a), plate 1. In the latter case it was observed that the free end sloped backward to the direction of its motion for the greater part of the cycle. This 'dragging' motion was shown (§ 5, part 1) to allow the cylinder to absorb energy from the fluid stream.

Buckling developed slowly with increasing flow velocity, and it was not always possible to determine the point of neutral stability accurately. The point of onset of oscillatory instabilities, on the other hand, was usually very clearly defined. According to linearized theory, of course, once the threshold of instability is crossed, the amplitude of motion should increase without limit. In fact, presumably because of non-linear effects not taken into account by theory, the maximum displacement in buckling and the amplitude of amplified oscillations were limited to usually one or two cylinder diameters. If the flow velocity was reduced below the point where oscillatory instability first occurred, the oscillation persisted with reduced amplitude; this also is an attribute of a non-linear system.

Transition from buckling to second-mode instability involved a gradual return of the cylinder to its position of rest along the x -axis, before further increase in the flow velocity resulted in unstable oscillation. (This agrees with the results shown in figure 5, part 1.) Increasing the flow velocity further at this point caused the amplitude and frequency of oscillation to increase, until the motion became erratic and the frequency was gradually reduced to nil; the cylinder then appeared to be buckled in its second mode. At this point, a small increase in the flow velocity precipitated third-mode, amplified oscillation of the system.

These observations showed the general behaviour of the system for increasing flow velocity to be in substantial agreement with theory (§ 4, part 1).

If the cylinder did not contain a metal strip which effectively limited its motion to the horizontal plane only, instability developed in one particular plane and, in the case of buckling, remained in this plane; amplified oscillation, on the other hand, soon degenerated into a three-dimensional motion, in which the plane of oscillation rotated slowly while the free end described a quasi-circular path.

Similar observations were made with a cylinder pinned at the upstream end and free at the other. The specific gravity of this cylinder was very nearly that of water ($\beta = 0.50$), so that gravity and buoyancy forces balanced almost exactly, making experiments in the horizontal plane feasible. The various instabilities occurred at lower flow velocities than for a similar cylinder with the upstream end clamped, and it was possible to observe fourth-mode amplified oscillation.

Considering pinned-pinned cylinders next, it was observed that, at small flow velocities, disturbances induced by small flow irregularities were damped quickly in this case also. If the cylinder was very flexible and long, it sagged slightly at its mid-point under its own weight. Increasing the flow velocity in such cases ex-

aggerated this sag and slowly shifted it to the horizontal plane, which was the preferred plane of motion. There was no distinct threshold for buckling instability. With increasing flow, the point of maximum lateral displacement moved downstream, as axial drag tended to put the downstream half of the cylinder in compression; eventually the cylinder became J-shaped, extending beyond the downstream support. No oscillatory instabilities developed.

On the other hand, if the cylinder was more resistant to axial extension, or if axial tension was applied at its ends, the behaviour of the system was much closer to that predicted by theory. In this case, for a sufficiently high flow velocity, a small bow developed just downstream of the mid-point of the cylinder, increasing in amplitude with flow, until it reached the maximum allowable by the extensibility of the cylinder. Increasing the flow further eventually caused spontaneous oscillation to develop, which was in form very much like second-mode vibration of the cylinder in still fluid (figure 2(b), plate 1); however, a travelling-wave component in the motion of the cylinder could be detected in the direction of flow, which is a requirement for the cylinder to absorb energy from the fluid stream, as predicted by the theory (§5, part 1). Further increase in the flow velocity caused both the frequency and amplitude of oscillation to increase. In some cases, for even higher flow velocities, third-mode unstable oscillation was observed.

Transition from buckling to second-mode oscillation involved a gradual shift of the position of maximum bow downstream, until a hump in the opposite direction appeared in the upstream half of the cylinder. The transition from this quasi-static condition to a fully unstable one necessitated a usually small, but finite, increase in the flow velocity.

(A ciné-film and a set of photographs are available showing the development of these instabilities and can be obtained by application to the author.)

4. The limits of stability

Sets of experiments were performed, each of which was designed to demonstrate the effect of varying one or more of the system parameters, while keeping all others as constant as possible.

The volumetric flow was measured with the aid of an orifice and the flow velocity was calculated assuming a uniform velocity distribution in the test section and taking account of the cross-sectional area occupied by the flexible cylinder. In each test, the flow velocity was increased in very small steps, noting the flow rates at which buckling and amplified oscillation developed spontaneously. In the latter case, the frequency of oscillation was also measured by visual counting. The values of m , D , L and EI were measured by straightforward methods not calling for comment, and M was taken to be equal to $\frac{1}{4}\pi D^2\rho$. From these measurements it was possible to evaluate the experimental, dimensionless, critical flow velocities for buckling u_{cb} and amplified oscillation u_{co} and the corresponding dimensionless frequency ω_{co} which is defined by

$$\omega_{co} = \{(M + m)/EI\}^{\frac{1}{2}} \Omega_{co} L^2,$$

where Ω_{co} is the circular frequency of oscillation.

To obtain the corresponding theoretical values of u_{cb} , u_{co} and ω_{co} , the system parameters must be known. Of these, β and ϵ may be calculated from the above measurements. For cylinders with the downstream end free, χ was determined by measuring the volume of the tapered end-piece. For cylinders with both ends pinned, the dimensionless tension parameter Γ was determined indirectly, by measuring the length of the extended cylinder *in situ* at zero flow velocity, with the aid of a travelling microscope. (It is recalled that $\Gamma = T_0 L^2/EI$, where T_0 is the flow-independent axial tension applied by axial movement of the downstream support. Calibration of length versus tension was obtained from simple extension tests in which the cylinder was horizontally submerged in a water tank, so that the effects of gravity and buoyancy were taken into account.) The experimental determination of the parameters c_N , c_T , c'_T and f was not attempted, however, which makes direct quantitative comparison between experiment and theory difficult.

The normal and longitudinal components of drag per unit length of a smooth cylinder inclined at angle i to the fluid stream were found by Taylor (1952) to be

$$F_N = \frac{1}{2}\rho DU^2(C_{Dp} \sin^2 i + C_N \sin^{\frac{3}{2}} i) \quad \text{and} \quad F_L = \frac{1}{2}\rho DU^2 C_T \cos i \sin^{\frac{1}{2}} i,$$

respectively, where $C_N = 4R^{-\frac{1}{2}}$ and $C_T = 5.4R^{-\frac{1}{2}}$ are the coefficients of friction drag, in the two directions, C_{Dp} is the coefficient of form drag, and R is the Reynolds number based on the free-stream velocity and cylinder diameter. For rough cylinders (turbulent boundary layers) Taylor proposed the following expressions:

$$F_N = \frac{1}{2}\rho DU^2(C_{Dp} \sin^2 i + C_f \sin i) \quad \text{and} \quad F_L = \frac{1}{2}\rho DU^2 C_f \cos i,$$

which for the purposes of the analysis of part I were linearized to

$$F_N = \frac{1}{2}c_N(MU^2/D) \sin i \quad \text{and} \quad F_L = \frac{1}{2}c_T MU^2/D,$$

in which c_N and c_T are not necessarily equal (if they are equal, then

$$c_N = c_T = \frac{4}{\pi} C_f).$$

The observed instabilities in the experiments to be described were generally in the range $10^4 < R < 10^5$. According to Fage & Warsap (1930), for reasonably smooth cylinders perpendicular to the flow ($k/D \leq 2 \times 10^{-3}$, k being the height of protrusions), the boundary-layer transition to turbulence occurs at $R > 10^5$. However, there is no evidence that these results apply to inclined cylinders at small angles of incidence. It may be argued that, for flexible cylinders subjected to small random motions where the inclination is a function of both position and time, transition to turbulence may occur at lower Reynolds numbers. Transition would be aided by minor mismatching at the upstream connexion of the flexible cylinder to the rigid support or tapered end-piece, as the case may be, which would act as a trip wire. It may be reasonable, therefore, to consider that, in the range of flow velocities where instabilities were observed, the boundary layer was turbulent over most of the cylinder. The linearized expressions for the components of drag used in part I may be expected to provide reasonable representation of the actual drag forces. Unfortunately, no experimental data

are available for estimating c_N and c_T . Accordingly, it was assumed that both c_N and c_T are approximately equal to $16/\pi R^{\frac{1}{2}}$, corresponding to $C_f \approx 4R^{-\frac{1}{2}}$, and for the purposes of comparison of experiment with theory, the 'representative' values of $c_N = c_T = 0.04$ and 0.02 were used.

In dealing with clamped-free cylinders, the values of the parameters f and c'_T were difficult to estimate and, accordingly, the experimental results were compared with theory for a number of values of f and c'_T . It is recalled that f is a measure of how closely the lateral forces over the tapered end-piece approach those given by two-dimensional, slender-body, inviscid flow theory. The optimum of $f = 1$ is obtained with a smoothly tapering elongated end-piece over which no separation takes place; clearly, the form drag coefficient c'_T then approaches zero. For less streamlined end-pieces, we have $f < 1$ and $c'_T > 0$. For all the end-pieces used, flow separation took place at some point, as evidenced by the introduction of air bubbles in the fluid stream, so that $f < 1$ and $c'_T > 0$ in all cases. (In part 1, the boundary conditions at the free end were lumped, on the assumption that the end-piece be short relative to the overall length of the cylinder. This conflicts with the requirements for $f = 1$, $c'_T = 0$ stated above, except in the limit for vanishing cylinder diameter.) For uniformity of presentation, the following arbitrary combinations of values of c'_T and f were used in the theoretical calculations for comparison with experiment: $f = 1$, $c'_T = 0$; $f = 0.8$, $c'_T = 0.2$; $f = 0.7$, $c'_T = 0.2$; and $f = 0.7$, $c'_T = 0.4$. Finally, since χ was always between 0.01 and 0.025 , and it has a very small effect on stability (§ 6, part 1), all calculations were done with $\chi = 0.01$.

Clamped-free cylinders

(a) Effect of the shape of the tapered end

A number of tests were conducted in which a cylinder ($D = 0.653$ in., $L = 15.4$ in., $m = 0.014$ lb./in., $EI = 859$ lb.in.³/sec²) was successively fitted with several tapered end-pieces, ranging from well-streamlined to blunt shapes. At the end of each test, the end-piece was removed and a new one glued in position. The sequence was repeated several times, in order to establish the effect of orientation and possible misalignment between the end-pieces and the cylinder.

The critical, dimensionless flow velocities for buckling u_{cb} and second-mode oscillation u_{co} are compared with the theoretical values for $c_N = c_T = 0.04$ in figure 3. The results for each end-piece cover a considerable range of u , indicating that small misalignments may have considerable effect on stability. The arrows indicate that the system was stable up to the maximum flow velocity of about 20 ft./sec attainable with the apparatus, corresponding to $u \approx 14$. Under such circumstances, 'stable' means that no distinct buckling or oscillation developed; nevertheless, there were damped, apparently random motions of irregular frequency and amplitude.

An ideally slender end is characterized by $f = 1$ and $c'_T = 0$ (§ 2, part 1), while for blunter ends $f < 1$ and $c'_T > 0$. According to theory, decreasing f stabilizes the system for buckling, while increasing c'_T destabilizes it. These conflicting

effects may be partly responsible for the results obtained for buckling. (Another reason is the difficulty in pinpointing the condition of neutral stability for buckling, which, unlike for unstable oscillation, was not always sharply defined.)

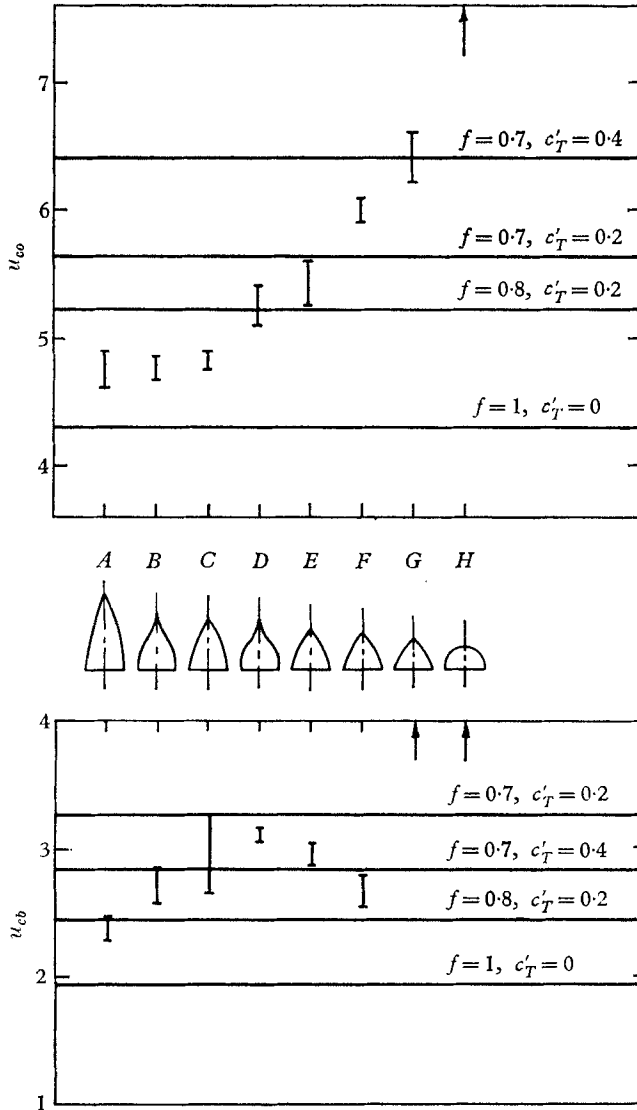


FIGURE 3. The effect of the shape of the tapered end-piece on stability of clamped-free cylinders; comparison of experiments, with theory ($c_N = c_T = 0.04$, $\chi = 0.01$, $\beta = 0.46$).

For second-mode instability, on the other hand, theory predicts that decreasing f and increasing c'_T both have a stabilizing effect. This is clearly supported by the experimental observations. If the cylinder was not fitted with a tapered end-piece, which corresponds to $f \rightarrow 0$, no instabilities were observed. For $c'_T = 0.4$

theory predicts that no buckling should occur when $f \leq 0.63$ and no second-mode instability when $f \leq 0.60$; this occurs at increasingly smaller values of f for larger values of c'_T . It should be noted that the qualitative agreement between experiment and theory would not be affected if the theoretical values were calculated for $c_N = c_T = 0.02$; the theoretical values would be generally smaller.

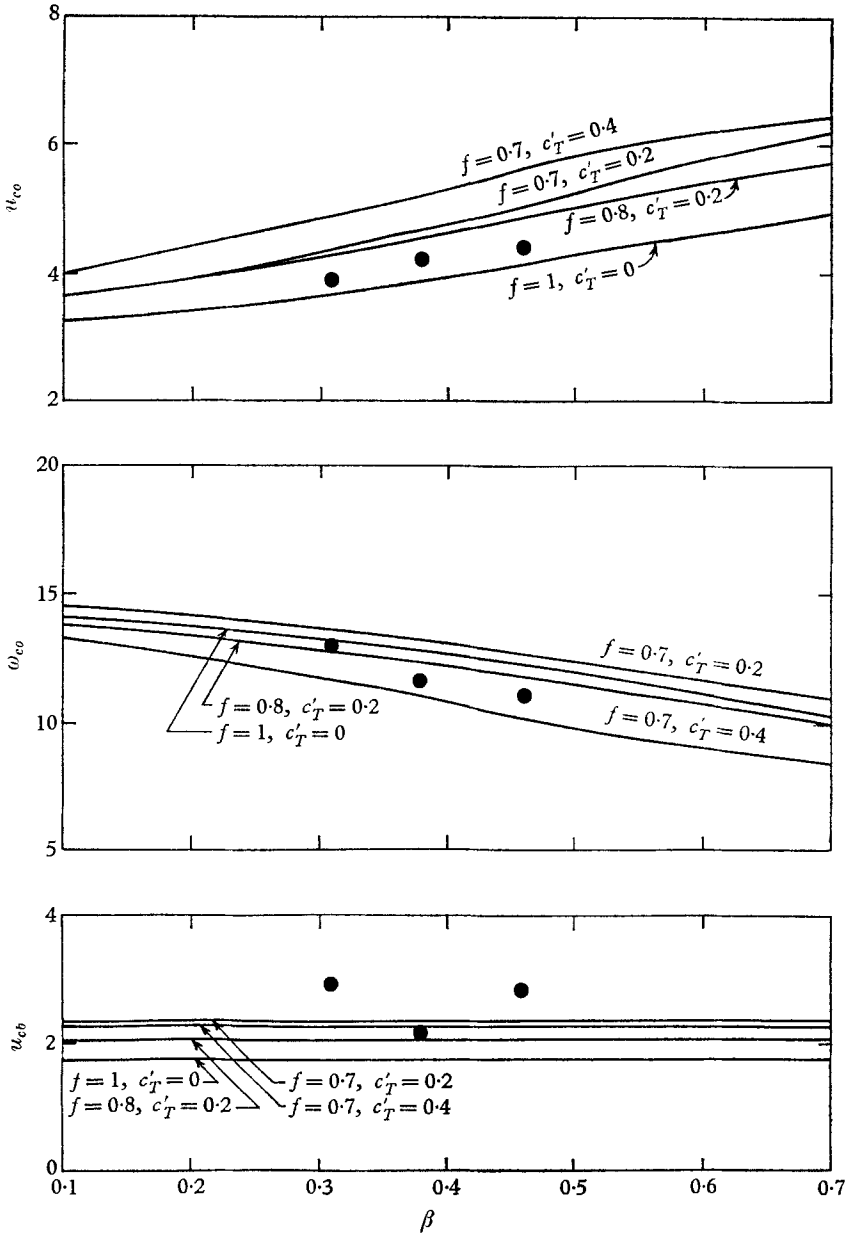


FIGURE 4. The effect of the mass ratio β on the stability of clamped-free cylinders; comparison of experiments, conducted with a 'smooth' cylinder, with theory ($c_N = c_T = 0.02$, $\chi = 0.01$).

Third-mode oscillatory instability was not greatly affected by the shape of the end-piece. In all these cases, it occurred at $7.1 < u < 8.5$, except with end-piece H , where it did not occur at all (for $u \leq 14$).

In all subsequent experiments, end-pieces similar in shape to B and C were used.

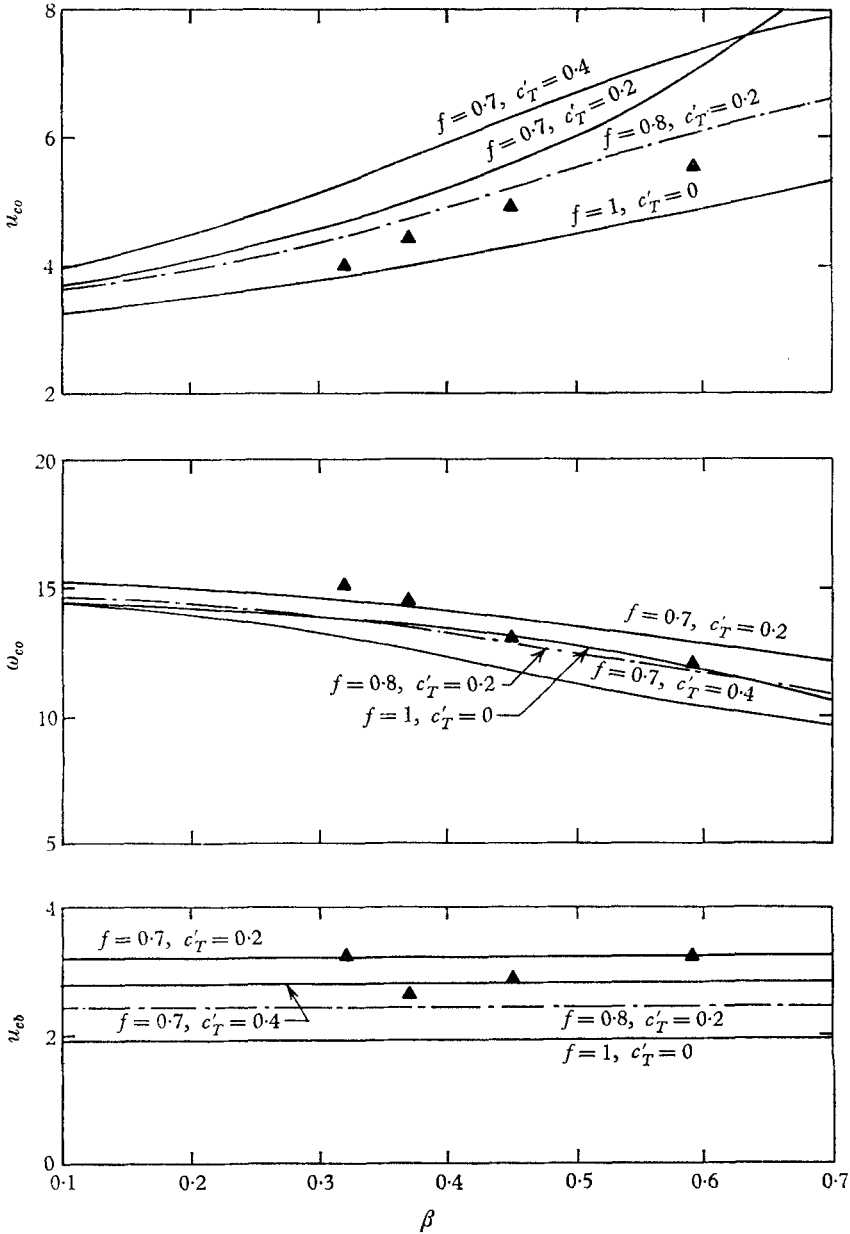


FIGURE 5. The effect of the mass ratio β on the stability of clamped-free cylinders; comparison of experiments, conducted with a 'rough' cylinder, with theory ($c_N = c_T = 0.04$, $\chi = 0.01$).

(b) Effect of the mass ratio β

Experiments in which β was varied were conducted with two hollow cylinders successively filled with various substances, such as air, water, sand, lead shot and mercury. One cylinder was cast and had a very smooth surface finish ($D = 0.665$ in., $L = 13.20$ in., $EI = 2600$ lb.in.³/sec²), while the other was constructed from small segments (§ 2) and was fairly rough ($D = 0.65$ in., $L = 14.7$ in., $EI = 1150$ lb.in.³/sec²). The two tapered end-pieces were almost identical. Both cylinders had steel strips in their central planes. Even so, it was found impossible to do successful experiments with $\beta < 0.3$, because the steel strip could not support the weight of the cylinder without twisting; if, on the other hand, the tube were made stiff enough to support itself, the flow necessary to destabilize the system exceeded the capacity of the available apparatus.

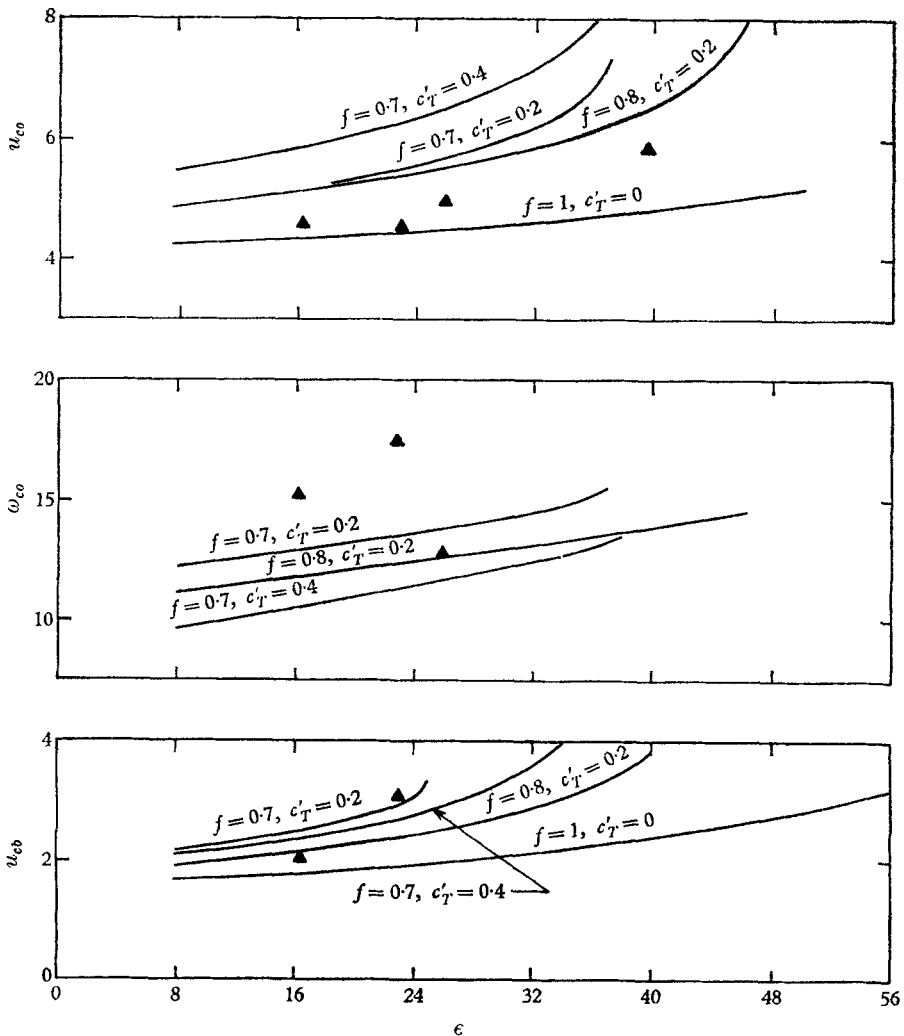


FIGURE 6. The effect of the slenderness ratio ϵ on the stability of clamped-free cylinders; comparison of experiments with theory ($\beta = 0.5$, $\chi = 0.01$, $c_N = c_T = 0.04$).

The experimental results for the 'smooth' and 'rough' cylinders are compared with the theoretical values for $c_N = c_T = 0.02$ and 0.04 , respectively, in figures 4 and 5. It is noted that in both cases u_{co} increases with β , and ω_{co} decreases, which is in qualitative agreement with theory; furthermore, comparison with the theoretical values in the envelope defined by $f = 1$, $c'_T = 0$ and $f = 0.7$, $c'_T = 0.2$ shows that quantitative agreement is also reasonably good. Agreement between experiment and theory in the case of buckling is not as good. The experimental results in this case show considerable variation with β , although theoretically there should be none.

(c) *Effect of surface roughness*

A number of experiments described above were repeated after the surface of the cylinder was roughened by rubbing with coarse sandpaper. In some cases, roughening had a small, yet definite, stabilizing effect on second-mode instability,

	Buckling u_{cb}	Amplified oscillation	
		u_{co}	ω_{co}
Without thread	2.9-3.2	5.25	12.0
With thread	2.7-3.2	6.9-7.5	9.8-12

TABLE 1

which is in qualitative agreement with the theory. The effect on buckling remained small and within the range of experimental error; the substantial stabilizing influence predicted by theory (figure 9, part 1) was not reproduced experimentally.

In one case, a fine cotton thread, 0.006 in. in diameter, was wrapped helically around the cylinder ($D = 0.575$ in., $L = 14.33$ in., $m = 0.00969$ lb./in., $EI = 1260$ lb.in.³/sec²). Its effect on stability is shown in table 1. (The increased uncertainty in the results for the cylinder with the thread reflects the more erratic mode of transition to instability.) These results appear to confirm the observations discussed above.

The thread was subsequently replaced by a number of equally spaced rubber rings $\frac{1}{2}$ in. inside diameter and $\frac{5}{8}$ in. outside diameter. No instabilities developed in this case, perhaps because of large-scale separation behind each ring.

(d) *Effect of the cylinder length*

A series of tests were conducted with one cylinder ($D = 0.60$ in., $m = 0.00982$ lb./in., $EI = 565$ lb.in.³/sec²), the length of which was successively reduced by cutting off pieces from the free end. The same tapered end-piece was used in all tests.

The experimental results are compared with theoretical values for

$$c_N = c_T = 0.04$$

in figure 6. The theoretical values for ω_{co} corresponding to $f = 1$, $c'_T = 0$ are very

close to those for $f = 0.8$, $c'_T = 0.2$ and are not shown for the sake of clarity. When $\epsilon > 24$ no buckling developed and when $\epsilon > 40$ there was no second-mode instability, at least with the maximum attainable flow velocity. At $\epsilon = 39.6$ the amplitude and frequency of oscillation were erratic, the latter vanishing occasionally while the cylinder retained an S-shape.

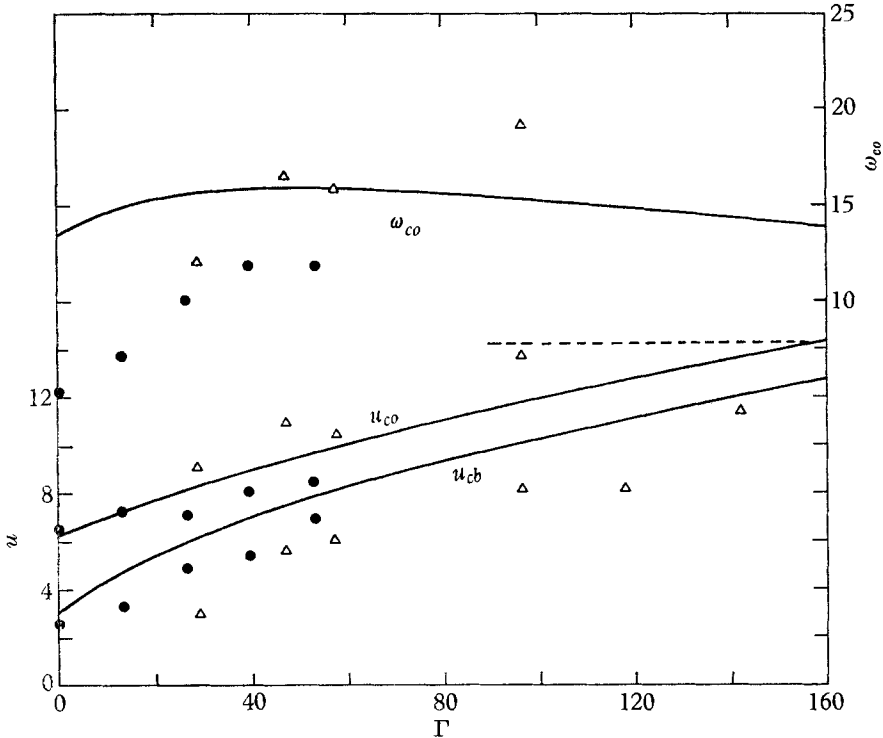


FIGURE 7. The effect of tension on stability of pinned-pinned cylinders; comparison of experiments with theory ($\beta = 0.48$; $ec_N = ec_T = 1$). Δ , cylinder A; \bullet , cylinder B.

In this case again, qualitative and, to a certain extent, quantitative agreement between experiment and theory for $0.7 < f < 1$ and $c_N = c_T = 0.04$ is reasonably good. Comparison with theory for $c_N = c_T = 0.02$ is less favourable; the rate of increase of u_{cb} and u_{co} with ϵ is considerably smaller in that case.

Pinned-pinned cylinders

A number of tests were conducted with cylinders hinged at both ends and subjected to varying uniform axial tension. As described before, the tension T_0 is applied by moving the supports apart and its value determined by measuring the extension of the cylinder. In experiments with cylinder A ($D = 0.53$ in., $L = 13.2$ in., $m = 0.00896$ lb./in., $EI = 365$ lb. in.³/sec²), T_0 ranged from 0.188 to 0.892 lb. Experiments in which the tension was smaller were not successful; the cylinder then sagged slightly before the flow was turned on and the behaviour of the system was as described in §3. Cylinder B ($D = 0.66$ in., $L = 13.0$ in., $m = 0.0138$ lb./in., $EI = 1033$ lb. in.³/sec²) was stiffer, and successful experiments with lower values of T_0 were possible.

The measured limits of stability are compared with the theoretical values of $\epsilon c_N = \epsilon c_T = 1$ (corresponding to $c_N = c_T = 0.04$ for cylinder *A*) in figure 7. On the scale of this figure the theoretical curves for $0 < \epsilon c_N = \epsilon c_T \leq 2$ are almost indistinguishable from those shown. For cylinder *A*, at $\Gamma = 118$ and 144 there was insufficient flow to cause second-mode instability (the dashed line corresponds to the maximum flow attainable). Agreement between experimental and theoretical critical flow velocities is generally within 25%. The discrepancy in the frequency of oscillation is much greater; no explanation for this can be advanced.

5. Conclusion

The experiments, conducted with apparatus of the simplest kind, demonstrated a number of phenomena which apparently have hitherto not been observed. The experiments appeared to confirm the essential features of the dynamical problem predicted by the theory developed in Part 1.

In general, it cannot be expected that the behaviour of the system with increasing flow velocity can be predicted by the linear analysis beyond the point where instability first occurs; the amplitude of motion then grows to the extent that forces not considered by the analysis come into play. It was particularly interesting, therefore, that the predicted oscillatory instabilities materialized as the flow velocity increased beyond the point where buckling occurred. The non-linear forces clearly have a limiting effect on the amplitude of motion.

Perhaps the most striking result, from the theoretical viewpoint, is the existence of oscillatory instabilities for cylinders with both ends supported, which was confirmed experimentally. It was shown in part 1 that instability in this case is caused specifically by frictional forces and that in the absence of hydrodynamic-drag effects only buckling is possible.

To test the effect on stability of proximity to the wall of the flow passage, one clamped-free cylinder was placed in turn in the $2\frac{1}{4}$ in. and 4 in. diameter test sections of the two test rigs. The differences in the measured limits of stability were within the range of experimental error.

A striking similarity was noted between the shape of fixed-free and pinned-free cylinders executing amplified oscillations and the swimming motions of long narrow animals (such as water snakes and eels) photographed by J. Gray (Taylor 1952). In the course of swimming motions the animal executes such motions that will propel it forward with minimum expenditure of energy; it is not surprising, therefore, that these motions are similar to those for which there is balance between expended and absorbed energy over a cycle, as in our case here.

The effect of the various dimensionless system parameters on stability demonstrated theoretically in part 1 was in some cases confirmed by experiment. Quantitative agreement between theory and experiment depends to a considerable extent on whether the assumption that c_N and c_T are not too different from 0.02 or 0.04 is correct. However, even when this is considered, it may be stated that the measured and calculated values of the limits of stability for second-mode unstable oscillation are in reasonably close agreement. In the case of clamped-free cylinders, this is true even if the measured values are compared with those for an

ideal end-piece, $f = 1$, $c'_T = 0$, excepting of course the experiments in which non-slender ends were purposely used. Agreement in the case of buckling is not nearly as good. However, bearing in mind the highly idealized nature of the theoretical model, closer agreement could hardly be expected.

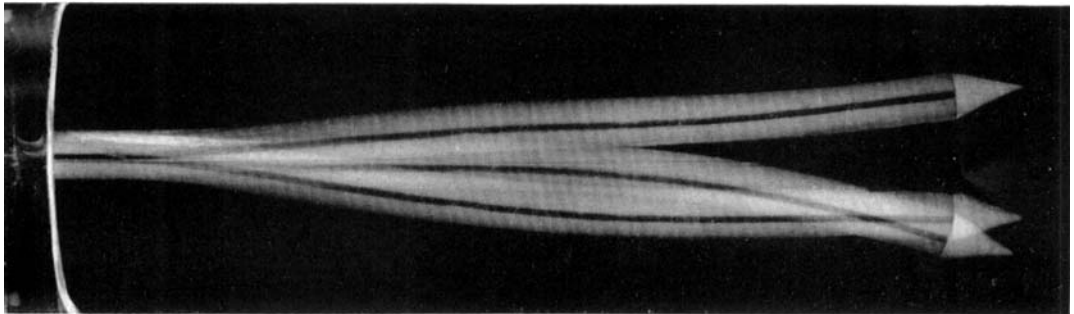
The analysis in the case of buckling instability provides a link with the theory of buckling of slender columns. When the cylinder is pinned at both ends, it is shown that, with increasing flow, buckling may occur at progressively smaller compressive loads than Euler's criterion requires, and for sufficiently large flow velocities it may occur under tension.

When the cylinder is clamped at the upstream end and free at the other, tension arising from form drag at the free end apparently destabilizes the system. Although increasing form drag causes buckling instability to be precipitated at smaller flow velocities, it is clear that it alone cannot cause buckling in the absence of flow. This aspect of the problem could fruitfully be investigated further.

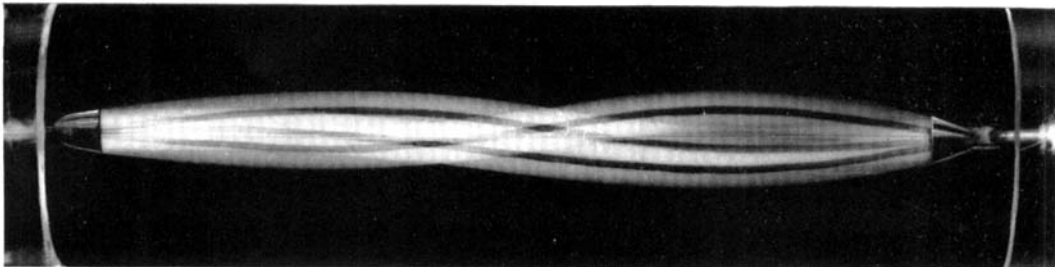
I am indebted to Mr F. L. Sharp for his assistance in conducting the experimental investigation.

REFERENCES

- FAGE, A. & WARSAP, J. H. 1930 *ARC R. & M.* no. 1283.
PAIDOUSSIS, M. P. 1966 *J. Fluid Mech.* **26**, 717.
TAYLOR, G. I. 1952 *Proc. Roy. Soc. A*, **214**, 158.



(a)



(b)

FIGURE 2. Second-mode amplified oscillation of (a) a clamped-free cylinder, and (b) a pinned-pinned cylinder in axial flow (multi-flash photographs). Flow is from left to right.